Research Article

Kumaravel Kaliaperumal, Kumaran Subramanian, Rajasekar Thirunavukkarasu, Ramesh Kumar Varadharajan, Reem Binsuwaidan, Nadiyah M. Alabdallah, Nawaf Alshammari, Mohd Saeed, Krishnan Anbarasu, and Rohini Karunakaran*

Antibacterial wound dressing with hydrogel from chitosan and polyvinyl alcohol from the red cabbage extract loaded with silver nanoparticles

https://doi.org/10.1515/gps-2023-0035
received February 27, 2023; accepted April 20, 2023

Abstract: The aim of the present study was the synthesis of hydrogel incorporated with chitosan blend with polyvinyl alcohol (PVA) from red cabbage *Brassica oleracea* and its application in wound healing and antibacterial activity. The chitosan/PVA hydrogel was synthesized by the combination of chitosan and PVA treated with acetic acid. The silver nanoparticles (AgNPs) were synthesized from the *B. oleracea* extract and its antibacterial efficacy was examined. The synthesized nanoparticles (NPs) were characterized using UV-spectroscopy and X-ray diffraction methods. The synthesized NPs were purified and combined with the hydrogel. This combined hydrogel and AgNP mixture was then subjected to Fourier transform infrared analysis, and the results were observed to conclude the effectiveness of the hydrogel. This hydrogel would differ in the part of dressing the wound, that is it can last on the wound for a longer period, thus reducing the pain and frequency of dressing and in turn naturally healing the wound in less time.

Keywords: nanomaterials, silver nanoparticle, PVA, red cabbage, *Brassica oleracea*

*** Corresponding author: Rohini Karunakaran,** Department of Biochemistry, Faculty of Medicine, AIMST University, Bedong, Malaysia; Department of Bioinformatics, Centre for Excellence for Biomaterials Science, AIMST University, Bedong, P.O. Box 08100, Malaysia; Department of Computational Biology, Saveetha School of Engineering, SIMATS, Chennai, India, e-mail: rohini@aimst.edu.my
Kumaravel Kaliaperumal: Unit of Biomaterials Research, Department of Orthodontics, Saveetha Dental College, SIMATS, Saveetha University, Chennai, Tamilnadu, India
Kumaran Subramanian, Rajasekar Thirunavukkarasu: Centre for Drug Discovery and Development, Sathyabama Institute of Science and Technology, Chennai, Tamilnadu, India
Ramesh Kumar Varadharajan: Department of Biotechnology, Sathyabama Institute of Science and Technology, Chennai, Tamilnadu, India
Reem Binsuwaidan: Department of Pharmaceutical Sciences, College of Pharmacy, Princess Nourah Bint Abdulrahman University, P.O. Box 84428, Riyadh 11671, Saudi Arabia
Nadiyah M. Alabdallah: Department of Biology, College of Science, Imam Abdulrahman Bin Faisal University, P.O. Box 1982, 31441, Dammam, Saudi Arabia; Department of Biology, Basic and Applied Scientific Research Centre, Imam Abdulrahman Bin Faisal University, P.O. Box 1982, Dammam 31441, Saudi Arabia
Nawaf Alshammari, Mohd Saeed: Department of Biology, College of Sciences, University of Hail, Hail 55476, Saudi Arabia
Krishnan Anbarasu: Department of Bioinformatics, Saveetha School of Engineering, SIMATS, Chennai, Tamilnadu, India

1 Introduction

The first line of defense for the human body is the skin, which can be easily damaged by trauma, surgery, and burns [1]. The skin acts as a protective barrier which is vital in preventing wounds [2]. An ideal clinical wound covering should have mechanical strength, flexibility, and the ability for wound exudate absorbance, and should not stick onto the surface of wounds [3]. Traditional wound dressings are still the best sellers in the market because the use of novel wound coverings, including foams, nanofibers, and hydrogels, is in high demand as they provide anti-infective, anti-inflammatory, and pro-wound healing properties [4]. Hydrogels have been used successfully in numerous biomedical applications and act as a substitute extracellular matrix in creating a moist environment to promote the wound-healing process [5–8]. Several methods have been used to fabricate hydrogels, such as using gamma and UV rays and the freeze–thaw process [9]. Different biopolymers have been used in the synthesis of the hydrogel wound dressing. For instance, chitosan and polyvinyl alcohol (PVA) are mostly used in hydrogels because of their biocompatibility, low price, and non-toxicity [10].

Recently, the nanocomposites have been prepared by the incorporation of some NPs such as Ag and ZnO into

biopolymers, and the resultant materials are used as a wound dressing [1]. Silver nanoparticles (AgNPs) have been chosen as the transporter for drug conveyance, particularly macromolecules because of their physical and chemical properties. From the specialized perspective, the positive charge and dissolvability of the silver in water are vital. An AgNP is a successful nanoparticle (NP) utilized to date. Chitins are polysaccharides obtained from exoskeletons of ocean creepy crawlies like crabs, shrimp, and so forth; chitosan is for the most part deacetylated polymer from *N*-acetyl glucosamine that can be obtained through the antacid deacetylation of the chitins. The primary units are β-(1,4)-connected D-glucosamine, and they build up with the amine bunches that are haphazardly acetylated. The amine and –OH moieties render the chitosan with numerous exceptional properties, making it very much applicable in many areas, and are also easily available for chemical reactions. These factors can cause interactions between the chitosan and the negatively charged surfaces in an aqueous environment or with the charged membrane of the microorganisms; moreover, the interactions are gaining more attention in the nanotechnology field. Chitosans are non-toxic, biocompatible, and biodegradable compounds that are approved by the Food and Drug Administration. In today's world, pharmaceutical research has mostly focused on the development of nanotechnological systems applicable in many different fields of medicine, especially in the field of drug delivery [9,11].

Currently, the application of biopolymers as NPs represents the other systems with a larger potential for the targeted transportation of drugs or the biological macromolecules inside the human body. Biopolymer NPs are effectively used to provide bioactive molecules for *in vivo* and *in vitro* functions. Nano biopolymers also show great use in enzyme replacement therapy. Naturally, the certainty of using the NPs synthesized by bio-compatible and bio-degradable polymers to distribute the enzymes in those tissues where they are missing or in complete absence represents a huge advantage in overcoming a series of ERT complications. More typically, nanotechnologies are an extended research stream, which is characterized by the use of materials with their sizes ranging from 1 to 1,000 nm. The application of these bio-polymers in medicine has coined the definition of "polymers therapeutics" to report different classes of nano compounds, at present, in the application as polymeric drugs, polymer–drug conjugates, polymer–protein conjugates, polymeric micelles, and polyplexes [12].

2 Methods

2.1 Chemicals

All the chemicals and reagents used in the present study were procured from Sigma Aldrich (USA). The chemicals used were of analytical grade (AR). The microbial strains were procured from Himedia, India which are of American-type cell culture (ATCC).

2.2 Extraction of pigments from red cabbage

The red cabbage (purple-leaved varieties of *Brassica oleracea*, *Capitata* group) is a kind of cabbage that is also known as Blaukraut after its preparation. Its leaves are colored dark in red/purple. However, the plant changes its color according to the pH value of the soil due to a pigment belonging to anthocyanins. In acidic soils, the leaves grow more reddish; in neutral soils, they grow purple; while an alkaline soil will produce greenish-yellow colored cabbages. The red cabbages were purchased from a market in Chennai, keeping in mind the freshness and quality of the cabbage. The cabbage was thoroughly washed with tap water and distilled water. With the help of a knife, the cabbages were cut into tiny pieces and these pieces were then ground into a paste texture with the solvent. The ground paste was then kept in a container for about 1 h for the pigments to get extracted thoroughly into the solute. After 1 h, the paste was filtered out into another clean and sterile container with the help of a clean cotton cloth. The extract was double-filtered using Whatman filter paper. The extract was kept for evaporation for concentrating. It was then poured into a Rotatory evaporator for the complete removal of the solvent from the extracted pigment [13].

2.3 Preparation of AgNPs

Due to their distinctive physicochemical characteristics, AgNPs have become one of the most appealing nanomaterials in recent years. AgNPs are synthesized through physical, chemical, and biological processes. AgNPs are mostly employed in the treatment of bacteria and cancer, in the promotion of bone and wound healing, as well as in vaccine adjuvants, anti-diabetic medications, and

biosensors. The size and shape of the AgNPs affect these special features. Physical properties like achieving uniform particle size distribution, identical shape, morphology, coating or stabilizing agents for NPs, chemical composition or type, and crystal structure are some of the main issues that must be controlled during the synthesis of AgNPs [14].

$AgNO_3$ was employed as the silver ion complex for the production of AgNPs. $AgNO_3$ was prepared in the dark and stored in a dark-brown bottle because the particles are light sensitive. The $AgNO_3$ solution was mixed with the red cabbage extract, and the mixture was left in the dark for a day. The $AgNO_3$ solution was prepared by adding 1.69 mg $AgNO_3$ in, 100 mL distilled water. AgNPs were synthesized by combining 90 mL of $AgNO_3$ and 10 mL of the red cabbage extract. The following day, it was kept in a water bath to provide heat and aid in the creation of AgNPs. The $AgNO_3$ crystals were dissolved in distilled water to prepare the $AgNO_3$ solution. The $AgNO_3$ solution was stored in a brown bottle and kept in a dark environment because it is sensitive to sunlight. The $AgNO_3$ solution contained the red cabbage extract, which was then left undisturbed for a day [15].

2.4 Synthesis of the polymer/hydrogel

PVA and chitosan were combined to synthesize the polymer. As shown in Figure 3, the chitosan solution was prepared by combining 1 g of chitosan powder with 50 mL of distilled water while stirring continuously over a magnetic stirrer to ensure that all of the particles completely dissolved in the water. Then, 50 mL of distilled water and 1 g of PVA were combined and swirled once more using a magnetic stirrer. After that, these two solutions were combined to obtain a single solution. A few drops of acetic acid were added to this solution. It was then kept over the magnetic stirrer for about 4 h for the complete mixing of the solution. The synthesized AgNPs were dissolved and mixed with the hydrogel thoroughly [16].

2.5 Hydrogel loaded with AgNPs

The synthesized AgNPs were then added to the chitosan and PVA hydrogel; distilled water was used to dilute the AgNP pellets for this. Next, this solution was added to the prepared hydrogel. The AgNP solution was added to 50 g of hydrogel, which is equal to 50 mL. The AgNPs and the hydrogel were completely blended on the magnetic stirrer for around 2 h [17].

2.6 Antibacterial activity

By using the well diffusion assay method in Petri plates containing the nutrient agar, the antibacterial activity of AgNPs was examined. *Pseudomonas aeruginosa* (ATCC 9027) and *Klebsiella pneumoniae* (ATCC BAA-1705) were used in the present study for the antibacterial screening assay. The plates containing 15 mL of nutrient agar were seeded with test bacterial cultures; the wells (6 mm diameter) were made with the help of a 6 mm diameter cork borer and the wells were loaded with control (distilled water) and AgNPs and were incubated at 37°C for 24 h. Distilled water was used as a negative control. After 24 h of incubation, the efficacy of the NPs is determined in terms of the zone of inhibition of the organism. The higher the zone of inhibition, the more the test sample will be effective [18]. Experiments were carried out in triplicate to obtain the mean value.

2.7 UV spectroscopy

The prepared AgNPs were characterized by UV spectroscopy. According to this technique, many molecules absorb UV light. The percentage of transmittance of light radiation is determined when the light of a certain frequency is passed through the samples. The synthesis of NPs in the solution was assessed by UV-visible (UV-Vis) scanning in the range of 200–700 nm in a spectrophotometer (Implen GmBH) using a quartz cuvette with water as the reference [19].

2.8 Fourier transform infrared (FTIR) spectroscopy

FTIR is a technique for obtaining an infrared spectrum of a solid, liquid, or gas's absorption or emission. The high-resolution spectral data are simultaneously gathered from an FTIR spectrometer over a variety of wavelengths. This has a substantial benefit over a dispersive spectrometer, which only measures the intensity over a small range of wavelengths at a time. A portable attenuated total reflectance FTIR analyzer from A2 Technologies (L1280127, Perkin Elmer, USA) was used to analyze an AgNP sample (ATRS-FTIR). For ten scans at room temperature, sample spectra were captured in the absorbance mode with a resolution of 4 cm in the middle infrared band between 4,000 and 400 cm^{-1} [11].

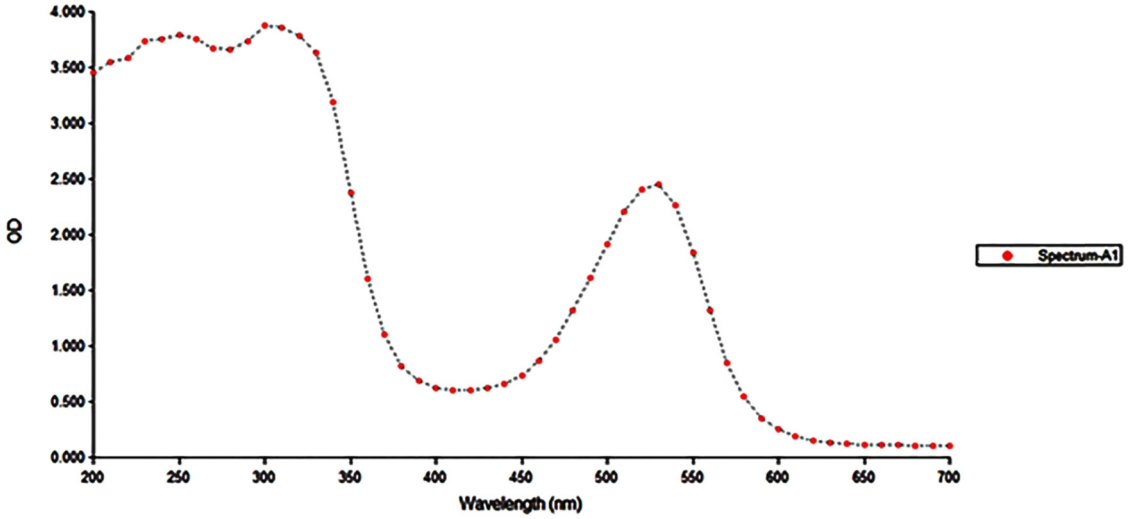

Figure 1: UV-Vis spectroscopy screening of AgNPs from *Brassica oleracea;* visible peaks are at 480 and 520 nm.

2.9 X-ray diffraction (XRD) analysis

XRD is the versatile dissipation of X-ray photons by particles in an occasional grid by utilizing Bragg's law:

$$n\lambda = 2d\sin\ \theta \tag{1}$$

XRD measurement was performed on an X'Pert Pro X-ray Diffractometer (Bruker, D8 Advance) operated at a voltage of 40 kV and a current of 30 mA with Cu Kα radiation. About 5 mg of AgNPs was placed on the glass side and placed over the space between the emission X-ray bar and reflecting beams. The X-rays emitted from the filament and passing through the powder sample reflecting emitted rays from the sample were collected. The sample was scanned at 2θ from 0 to 90°, and the X-ray peaks were evaluated with JCPDS database values [20].

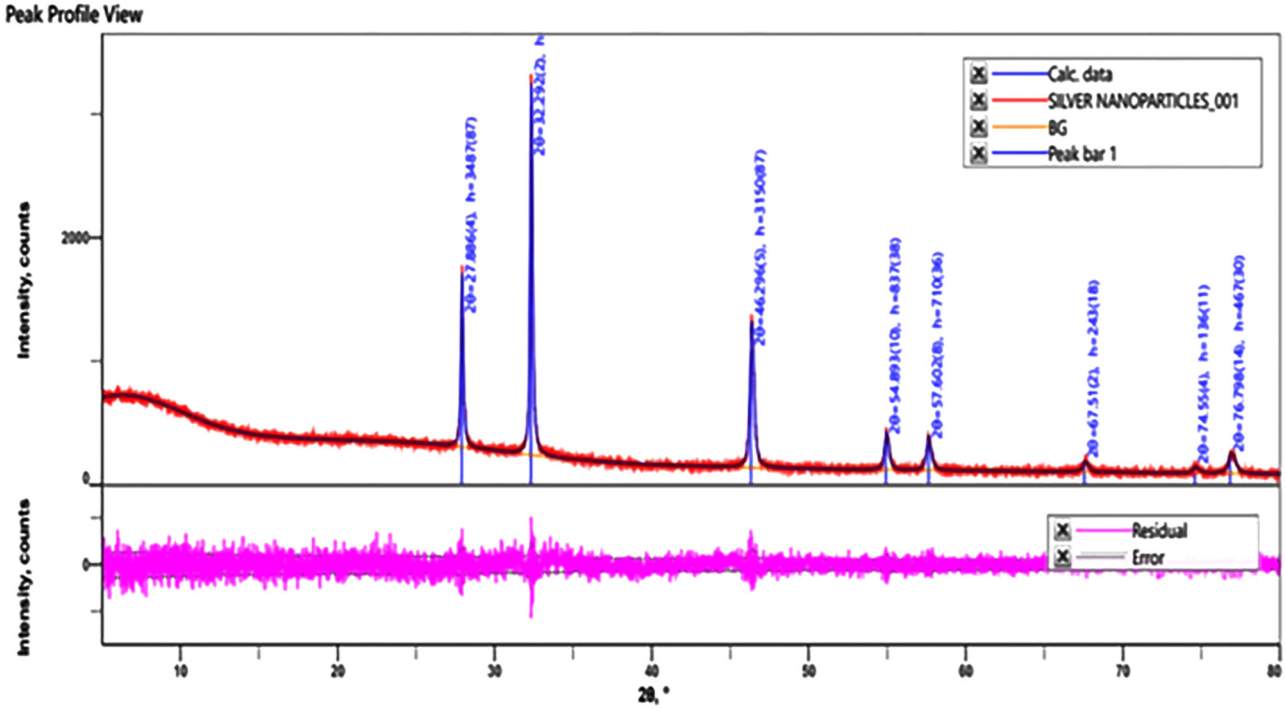

Figure 2: XRD pattern of the synthesized AgNPs.

3 Results

3.1 Ag NP characterization

UV spectra of AgNPs were recorded and are shown in Figure 1. The AgNP formation was confirmed by UV-Vis spectroscopy. Every element has free electrons, which give rise to an absorption peak. This peak is dependent on the size and shape of the NPs formed. The formation of the AgNP was observed once every hour to confirm the exact time taken for the synthesis of AgNPs. The peak was found at 540 nm after 3 h.

The regular XRD pattern of the synthesized AgNPs is shown in Figure 2. The peak places of the pattern were affirmed by the VELS Institute of Science, Technology & Advanced Studies (VISTAS), Chennai. Further, no other polluting influence crest was seen in the XRD design, demonstrating the single-stage test arrangement. The diffracted intensities were recorded from 0 to 80°. Four strong Bragg reflections were seen at 32.29°, 46.26°, 67.51°, and 76.79° corresponding to the planes (111), (200), (220), and (311), respectively. The interplanar spacing values are 2.7700, 1.9595, 1.3864, and 1.24014, respectively. The crystalline size is calculated by the Debye–Scherrer formula

$$D = \frac{k\lambda}{\beta \cos\ \theta} \tag{2}$$

The calculated average crystallite of AgNPs is ~25 nm.

3.2 Particle size and zeta potential measurement

Particle size analysis was carried out to determine the size of produced AgNPs. It displays the dimensions of artificial AgNPs. Zeta potential analysis was used to assess the stability of AgNPs that had been produced. It primarily serves to stabilize NP dispersion. The estimated average zeta potential value of +50 mV indicates that the produced NPs are stable. This indicates a positive value, indicating that the positively charged AgNPs are coated with components that repel one another, preventing aggregation and maintaining the stability of the NPs. The particle size distribution curve yielded an average diameter of 724 nm (Figure 3). The zeta potential for the comparable value was found to be 11.1 mV. With 10 kV·m^{-1}, the AgNPs' polarity was found to be positive.

3.3 Characterization of hydrogels with AgNPs.

The potential functional groups present in the synthesized AgNPs were identified using the FTIR analysis. Major peaks in the FTIR spectrum were observed at 3,853, 2,090, 433, 422, 416, and 410 cm^{-1}. They were compared to the bond angles extending C–S linkage–H stretching–O–C group–H bond, alkyl ketone, alkane group, and aromatics group. The FTIR spectra of AgNPs were recorded. The main IR band of pure Ag is shown in Figure 4.

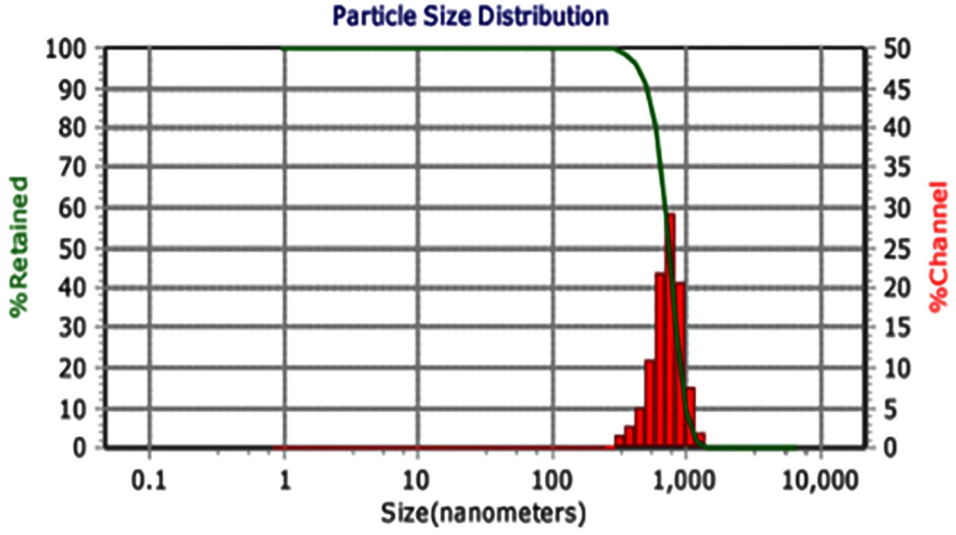

Figure 3: Particle size distribution of AgNPs. The average diameter determined by the particle size distribution curve is ~724 nm. The corresponding zeta potential value was found to be 11.1 mV. The polarity of the AgNPs is found to be positive with 10 kV·m^{-1}.

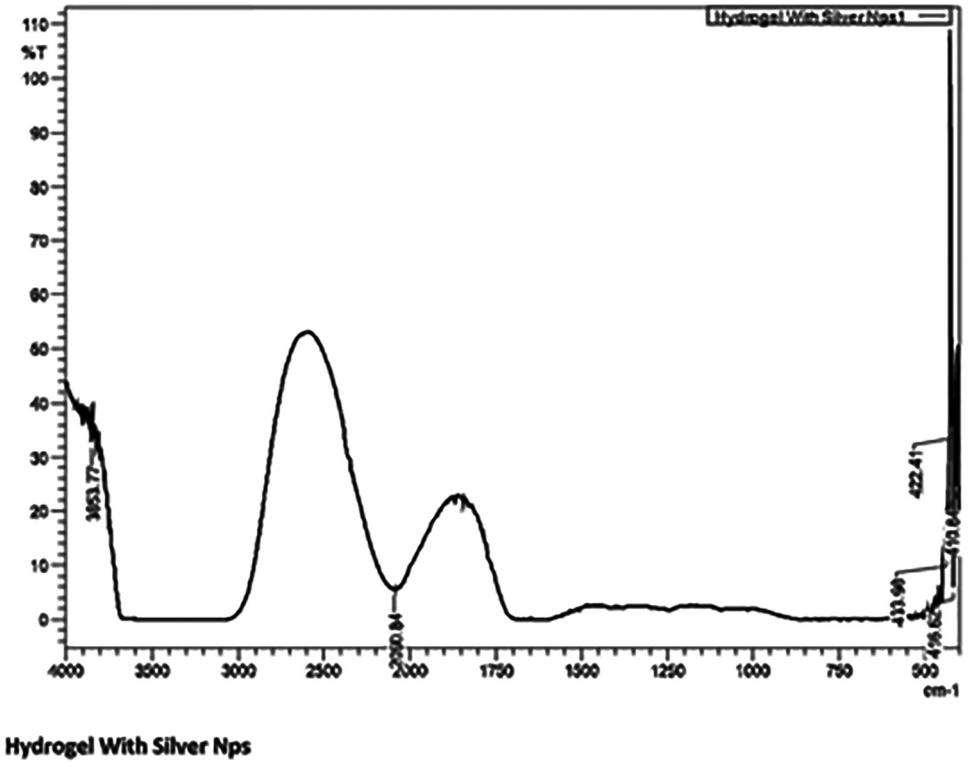

Figure 4: FTIR analysis peaks of hydrogel with AgNPs.

3.4 Antibacterial activity

The antibacterial test for AgNPs was conducted against two bacterial strains, namely *P. aeruginosa* and *K. pneumonia*. The well diffusion method was used for the detection of the antibacterial activity. Two agar plates were prepared. The bacterial solution was swabbed over the agar by a sterile cotton swab; this method of spreading the bacteria evenly over the agar plate is known as the method of swabbing. Wells were made, and the AgNP solution was added to the well to check its antibacterial activity. The entire assay was done in triplicate, and the standard error values obtained were tabulated (Table 1).

4 Discussion

The physicochemical properties of NPs are important for their behavior, bio-distribution, safety, and efficacy. Therefore, the characterization of AgNPs is important to evaluate the functional aspects of the synthesized particles [21]. The absorption of AgNPs depends on the particle size, dielectric medium, and chemical surroundings [22,23]. The observed peak was assigned for various metal NPs with sizes ranging from 2 to 100 nm [24]. The color change was observed by comparing it with the extract. In this study, *Brassica oleracea* has shown a similar peak range in the preliminary screening with UV spectroscopy. To achieve the optimal form and the size of NPs, various amounts of extract from different plants have been employed. The peak absorbance in the UV-Vis spectrum increased in the current study as the plant density increased. Furthermore, the particle size was decreased when more extract was used.

Two solutions were combined to obtain one solution to prepare the hydrogel: the first solution contained chitosan and distilled water, and the other contained PVA and distilled water. The solution was centrifuged and the AgNPs were collected. A previous report showed that an increase in the ZnO NPs increased the gel content, which varied between 60% and 87% [1]. The size of Ag NPs at the selected concentration was 1,010 nm and the zeta potential was 50 mV. All the analyses confirmed the effectiveness and efficiency of the hydrogel enriched with the AgNPs.

Table 1: Effects of AgNPs against the bacteria were observed and a positive result was obtained for both bacterial strains

S. no.	Microbes	Zone of inhibition (mm)
1.	*Pseudomonas* sp.	5 ± 0.025
2.	*Klebsiella* sp.	8 ± 0.0417

The antibacterial test for AgNPs was conducted against two bacterial strains, namely *P. aeruginosa* and *K. pneumonia*. The well diffusion method was used for the detection of the antibacterial activity. The FTIR analysis was used to determine the possible functional groups present in the synthesized AgNPs. The FTIR spectra showed major peaks at 3,853, 2,090, 433, 422, 416, and 410 cm^{-1}. No polluting influence crest was seen in the XRD design, demonstrating the single-stage test arrangement. The XRD peaks were seen located at 2θ = 27.8°, 32.2°, 46.2°, 54.8°, 57.6°, 67.5°, 74.5°, and 76.7°. Dynamic light scattering was used to measure the hydrodynamic diameter in the nm range. These results agree with those presented by researchers who have reported that Gram-positive bacteria are less susceptible to the antimicrobial activity of silver [25–28]. Grigor'eva et al. [29] investigated the cell responses to AgNPs for *Staphylococcus aureus* and *Salmonella typhimurium*. According to this study, the *S. typhimurium* culture that was incubated with AgNPs for the same period sustained slightly less overall damage than the *S. aureus* culture. Goswami et al. [30] showed that *Escherichia coli* was found to have a broader zone of inhibition and lower minimum bactericidal concentration and minimum inhibitory concentration (MIC) values when compared to *Bacillus subtilis*. The lower MIC values for *E. coli* were evaluated against *S. aureus* as per the report of Martinez-Castanon et al. [31]. In addition, Kim et al. [27] demonstrated that AgNPs inhibit *E. coli* at low concentrations, although their effects on *S. aureus* development were minimal. According to Tian et al. [32], AgNPs can induce wound healing with lessened scar formation and reduce inflammation through cytokine regulation. Moreover, Frankova et al. [33] provided evidence that human dermal keratinocytes in the AgNP-treated group released fewer growth factors and inflammatory cytokines (which are released by immune cells). Our research demonstrated AI-AgNPs' potential for bacterial cell disruption, which when combined with its capacity to scavenge free radicals, can be used to prepare wound dressings.

5 Conclusion

The main aim of the work is to prepare a wound-healing bandage formulated with chitosan and PVA with red cabbage extract loaded with AgNPs. The developed bandage impregnated with AgNPs was found to be effective in antibacterial properties showing significant antibacterial effects against *P. aeruginosa* and *K. pneumonia* bacterial strains. These bacteria are the major secondary infection-causing agents for most human ailments like respiratory diseases. The physicochemical properties of the AgNPs synthesized were significant in terms of zeta potential and chemical nature. As a future development, this chitosan and PVA-loaded AgNP-impregnated wound bandage can be tested by an *in vivo* animal wound model and further clinical tests for future product development.

Acknowledgments: We thankful much to the Department of Pharmaceutical Sciences, College of Pharmacy, Princess Nourah bint Abdulrahman University, P.O.Box 84428, Riyadh 11671, Saudi Arabia for for research supporting project number (PNURSP2023R304) for this research work.

Funding information: This research was funded by Princess Nourah bint Abdulrahman University Researchers Supporting Project number (PNURSP2023R304), Princess Nourah bint Abdulrahman University, Riyadh, Saudi Arabia.

Author contributions: Kumaravel Kaliaperumal, Kumaran Subramanian: writing – original draft, writing – review and editing, formal analysis; Ramesh Kumar Varadharajan, Rajasekar Thirunavukkarasu: writing – original draft, formal analysis; Reem Binsuwaidan, Nadiyah M. Alabdallah, Nawaf Alshammari: visualization, project administration; Mohd Saeed, Krishnan Anbarasu: supervision, conceptualization, writing – reviewing and editing; Rohini Karunakaran: resources.

Conflict of interest: The authors state no conflict of interest.

Data availability statement: All data generated or analyzed during this study are included in this published article.

References

[1] Khorasani MT, Joorabloo A, Moghaddam A, Shamsi H, Mansoori, Moghadam Z. Incorporation of ZnO nanoparticles into heparinized polyvinyl alcohol/chitosan hydrogels for wound dressing application. Intern J Biol Macromol. 2018;114:1203–15.

[2] Fan L, Yang H, Yang J, Peng M, Hu J. Preparation and characterization of chitosan/gelatin/PVA hydrogel for wound dressings. Carbohy Polymers. 2016;146:427–34.

[3] Jayakumar R, Prabaharan M, Kumar PS, Nair S, Tamura H. Biomaterials based on chitin and chitosan in wound dressing applications. Biotech Adv. 2011;29(3):322–37.

[4] Rath G, Hussain T, Chauhan G, Garg T, Goyal AK. Development and characterization of cefazolin-loaded zinc oxide

nanoparticles composite gelatin nanofiber mats for post-operative surgical wounds. MaterSciEng: C. 2016;58:242–53.
[5] Khorasani MT, Joorabloo A, Adeli H, Mansoori-Moghadam Z, Moghaddam A. Design and optimization of process parameters of polyvinyl (alcohol)/chitosan/nano zinc oxide hydrogels as wound healing materials. Carbohydr Polym. 2019;207:542–54. doi: 10.1016/j.carbpol.2018.12.021.
[6] Supare V, Wadher K, Umekar M. Experimental design: Approaches and applications in development of pharmaceutical drug delivery system. JDDT. 2021;15:154–61.
[7] Winter RE, Kolodziej SA, Lewis WH. Wound-healing composition and method. US Pat., WO98/35695, 1998.
[8] Jahani-Javanmardi A, Sirousazar M, Shaabani Y, Kheiri F. Egg white/poly (vinyl alcohol)/MMT nanocomposite hydrogels for wound dressing. J Biomater Sci Polym Ed. 2016;27(12):1262–76. doi: 10.1080/09205063.2016.1191825.
[9] Aljebory AM, Alsalman TM, Aljebory A, Alsalman TM. Chitosan nanoparticles: review article. Imp J Interdiscip Res (IJIR). 2017;3(7):233–42.
[10] Kalantari K, Afifi AM, Jahangirian H, Webster TJ. Biomedical applications of chitosan electrospun nanofibers as a green polymer- Review. Carbohydr Polym. 2019;1(207):588–600.
[11] Deepa B, Ganesan V. Bioinspired synthesis of selenium nanoparticles using flowers of *Catharanthus roseus* (L.) G. Don. and *Peltophorum pterocarpum* (DC.) Backer ex Heyne–a comparison. Inter J Chem Tech. 2015;7:725–33.
[12] Duncan R. Polymer therapeutics as nanomedicines: new perspectives. CurropinBiotech. 2011;22:492–501.
[13] Valencia-Arredondo JA, Hernández-Bolio GI, Cerón-Montes GI, Castro-Muñoz R, Yáñez-Fernández J. Enhanced process integration for the extraction, concentration, and purification of di-acylated cyanidin from red cabbage. Sep Purif Technol. 2020;238:116492.
[14] Salleh A, Fauzi MB. The in vivo, in vitro and in-ovo evaluation of quantum dots in wound healing: A review. Polymers. 2021;13:191. doi: 10.3390/polym13020191.
[15] Saravanan M, Barik SK, Mubarak Ali D, Prakash P, Pugazhendhi A. Synthesis of silver nanoparticles from *Bacillus brevis* (NCIM 2533) and their antibacterial activity against pathogenic bacteria. Microb Pathog. 2018;116:221–6.
[16] Kalantari K, Mostafavi E, Saleh B, Soltantaba P, Webster TJ. Chitosan/PVA hydrogels incorporated with green synthesized cerium oxide nanoparticles for wound healing applications. Eur Polym J. 2020;134:109853.
[17] Piras CC, Mahon CS, Smith DK. Self-assembled supramolecular hybrid hydrogel beads loaded with silver nanoparticles for antimicrobial applications. Chemistry (Weinheim an der Bergstrasse, Germany). 2020;26(38):8452–7. doi: 10.1002/chem.202001349.
[18] Fardsadegh B, Vaghari H, Mohammad-Jafari R, Najian Y, Jafarizadeh-Malmiri H. Biosynthesis, characterization and antimicrobial activities assessment of fabricated selenium nanoparticles using Pelargonium zonale leaf extract. Green Process Synthe. 2019;8(1):191–8. doi: 10.1515/gps-2018-0060.
[19] Wadhwani SA, Gorain M, Banerjee P, Shedbalkar UU, Singh R, Kundu GC, et al. Green synthesis of selenium nanoparticles using *Acinetobacter* sp. SW30: optimization, characterization, and its anticancer activity in breast cancer cells. Int J Nanomed. 2017;12:6841–55. doi: 10.2147/IJN.S139212.
[20] Dorofeev GA, Streletskii AN, Povstugar IV, Protasov AV, Elsukov EP. Determination of nanoparticle sizes by X-ray diffraction. Colloid J. 2012;74:675–85.
[21] Zhang XF, Liu ZG, Shen W, Gurunathan S. Silver nanoparticles: synthesis, characterization, properties, applications, and therapeutic approaches. Int J Mol Sci. 2016;17(9):1534. doi: 10.3390/ijms17091534.
[22] Nath SS, Gope DG. Synthesis of CdS and ZnS quantum dots and their applications in Electronics. Nano Trends. 2007;2:20–8.
[23] Noginov MA, Zhu G, Bahoura M, Adegoke J, Small C, Ritzo BA, et al. The effect of gain and absorption on surface plasmons in metal nanoparticles. Appl Phys B. 2007;86:455–60.
[24] Sastry M, Patil V, Sainkar SR. Electrostatically controlled diffusion of carboxylic acid derivatized silver colloidal particles in thermally evaporated fatty amine films. J Phys Chem B. 1998;102:1404–10. doi: 10.1021/jp9719873.
[25] Egger S, Lehmann RP, Height MJ, Loessner MJ, Schuppler M. Antimicrobial properties of a novel silver-silica nanocomposite material. Appl Env Microbiol. 2009;75(9):2973–6. doi: 10.1128/AEM.01658-08.
[26] Kawahara K, Tsuruda K, Morishita M, Uchida M. Antibacterial effect of silver-zeolite on oral bacteria under anaerobic conditions. Dent Mater. 2000;16:452–5. doi: 10.1016/S0109-5641(00)00050-6.
[27] Kim JS, Kuk E, Yu KN, Kim JH, Park SJ, Lee HJ, et al. Antimicrobial effects of silver nanoparticles. Nanomedicine. 2007;3(1):95–101. doi: 10.1016/j.nano.2006.12.001.
[28] Pal S, Tak YK, Song JM. Does the antibacterial activity of silver nanoparticles depend on the shape of the nanoparticle? A study of the Gram-negative Bacterium *Escherichia coli*. Appl Env Microbio 2007;73:1712–20.
[29] Grigor'eva A, Saranina I, Tikunova N, Safonov A, Timoshenko N, Rebrov A, et al. Fine Mechanisms of the interaction of silver nanoparticles with the cells of *Salmonella typhimurium* and *Staphylococcus aureus*. Biometals. 2013;26:479–88.
[30] Goswami AM, Sarkar TS, Ghosh S. An ecofriendly synthesis of silver nano-bioconjugates by *Penicillium citrinum* (MTCC9999) and its antimicrobial effect. AMB Express. 2013;3:16.
[31] Martinez-Castanon G, Nino-Martinez N, Martinez-Gutierrez F, Martinez-Mendoza J, Ruiz F. Synthesis and antibacterial activity of silver nanoparticle with different sizes. J Nano Res. 2008;10:1343–8.
[32] Tian J, Wong K, Ho CM, Lok CN, Yu WY, Che CM. Topical delivery of silver nanoparticles promotes wound healing. Chem Med Chem. 2007;2:129–36.
[33] Frankova J, Pivodova V, Vágnerova H, Juranova J, Ulrichova J. Effects of silver nanoparticles on primary cell cultures of fibroblasts and keratinocytes in a wound-healing model. J Appl Biomater Funct Mater. 2016;14:e137–42. doi: 10.5301/jabfm.5000268.